Faceting ionic shells into icosahedra via electrostatics

Graziano Vernizzi* and Monica Olvera de la Cruz*†‡

Departments of *Materials Science and Engineering and †Chemistry, Northwestern University, Evanston, IL 60208

Edited by Paul M. Chaikin, New York University, New York, NY, and approved September 27, 2007 (received for review April 16, 2007)

Shells of various viruses and other closed packed structures with spherical topology exhibit icosahedral symmetry because the surface of a sphere cannot be tiled without defects, and icosahedral symmetry yields the most symmetric configuration with the minimum number of defects. Icosahedral symmetry is different from icosahedral-shaped structures, which include some large viruses, cationic–anionic vesicles, and fullerenes. We present a faceting mechanism of ionic shells into icosahedral shapes that breaks icosahedral symmetry resulting from different arrangements of the charged components among the facets. These self-organized ionic structures may favor the formation of flat domains on curved surfaces. We show that icosahedral shapes without rotational symmetry can have lower energy than spheres with icosahedral symmetry caused by preferred bending directions in the planar ionic lattice. The ability to create icosahedral shapes without icosahedral symmetry may lead to the design of new functional materials. The electrostatically driven faceting mechanism we present here suggests that we can design faceted polyhedra with diverse symmetries by coassembling oppositely charged molecules of different stoichiometric ratios.

membranes | self-assembly | amphiphiles | buckling

One of the greatest challenges of modern biotechnology is understanding how to control the assembly of molecules into functional units (1, 2). A beautiful way in which nature develops functionality is by the diversity of shapes (3). Metallic nanocrystals (4) have various well studied shapes. Closed shapes in self-assembled soft-matter simple systems, including shells such as viral capsids (5), vesicles (6, 7), and emulsions (8), as well as micelles (9, 10), are understood in uncharged components systems. However, because symmetry has its roots in molecular interactions, charged molecules may form a large variety of self-assembled closed shapes, with potentially complex symmetries. Closed shapes (shells) allow segregation of components into confined microenvironments and thus can provide the right conditions for important self-catalytic biomolecular reactions (11). Moreover, in emulsions, the interface of immiscible liquids can adsorb macromolecules (12) that can facilitate both biological and biotechnological processes (13). Charged molecules readily accumulate at interfaces when positive and negative charges are coadsorbed to avoid charge accumulation. These interfaces may form ionic crystalline structures on flat (14), cylindrical (15), and spherical surfaces. However, unlike cylindrical and toroidal aggregates, spherical cationic–anionic emulsions and membranes cannot form defect-free structures over a sphere and thus may form faceted structures.

The shapes that amphiphilic molecules form are determined mainly by the aggregate's elastic properties, including bending rigidities, spontaneous curvature, and surface tension. Fluid amphiphilic membranes and emulsions cannot form faceted polyhedra. Fluid membranes cannot support a buckling transition, which—in elastic theory—is responsible for the faceting of tethered membranes or crystalline viral shell capsids (16). Indeed, other forces are required to change the shape of nontethered amphiphile spherical emulsions and membranes. In amphiphilic systems, for example, faceted closed structures can arise by mixing oppositely charged amphiphiles (17). Although the role of electrostatic interactions in the self-organization of atomic systems into ionic crystals is well understood, the effect of electrostatics in ionic amphiphilic membranes or emulsions has not been fully studied. In this paper, we demonstrate that electrostatic interactions are able to change the shape of closed spherical ionic shells, such as emulsion or lipid membranes, into icosahedral shapes via a unique faceting mechanism.

In nature there are many examples of spherically closed packed structures that take symmetries on the sphere with the largest symmetry group, that is icosahedral symmetry (18, 19). In this respect icosahedral symmetry is ubiquitous. However, icosahedral shape is much less common. Icosahedral-shaped structures can have interesting experimental properties, including the ability to template patterns on the surface or allow recognition of specific locations (e.g., during phage assembly). Further, icosahedral symmetry and icosahedral shape are related but not synonymous. Systems can have icosahedral symmetry but not icosahedral shape and vice versa. For instance, intermediate viruses display icosahedral symmetry but not icosahedral shape. Instead, as shown here, a stoichiometric system of charges distributed optimally over an icosahedron inevitably breaks icosahedral symmetry.

The physical origin of icosahedral symmetry, and the prediction of the "quasi-equivalent" triangulations of the icosahedron (5), have been derived from the energy minimization of a thermodynamical system of particles on a sphere with short-range interactions (19). The quasi-equivalent triangulations are all possible regular triangulations, with only 12 5-fold disclinations at the vertices of the icosahedron. They are labeled by a pair of integer numbers (a, b), which are the coordinates of an edge joining two nearest icosahedral vertices, with respect to the basis $(\boldsymbol{a}, \boldsymbol{b})$ of the hexagonal closed-packed lattice (see Fig. 1). Once this edge is fixed, all of the 20 faces are uniquely determined. The total number of the triangles is $20T$, and the total number of vertices (that is, the number of particles) is $n = 10T + 2$, where $T = a^2 + b^2 + ab$ is the number of triangles per icosahedral face, and it assumes only certain values, $T = 1, 3, 4, 7, 9, 12, 13, 16, 19, 21 \ldots$ (some examples are shown in Figs. 1 and 2).

On the other hand, the origin of icosahedral shape has been explained by the continuum elastic theory of buckling (16, 20, 21). The theory shows how a thin elastic spherical shell "buckles" into an icosahedral shape when its Foppl–von Kármán number $\gamma = Y R^2/\kappa$ is larger than a critical value (16), where Y is the Young's modulus of the shell, κ is the bending rigidity, and R is the linear size of the shell. The seeds of the buckling are 12 5-fold disclinations that are assumed to be positioned at the vertices of an icosahedron. Therefore the icosahedral symmetry of defects on a sphere is a necessary condition, but not sufficient, for buckling.

Here we describe a mechanism, not based on continuum elastic theory, that leads to icosahedral shapes and, more generally, their faceting into polyhedra. Such a mechanism involves electrostatic interactions in coassemblies of oppositely

Author contributions: G.V. and M.O.d.l.C. designed research, performed research, and wrote the paper.

The authors declare no conflict of interest.

This article is a PNAS Direct Submission.

‡To whom correspondence should be addressed. E-mail: m-olvera@northwestern.edu.

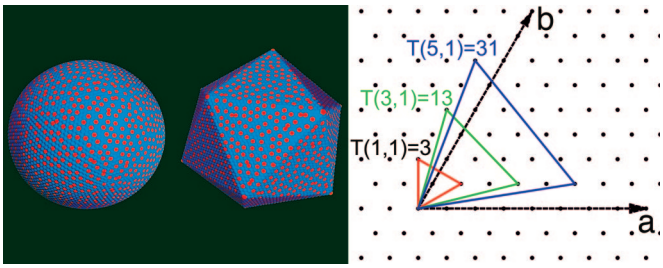

Fig. 1. A snapshot of an unrelaxed distribution of positive and negative charges over a sphere and an icosahedron (*Left*). The triangular lattice on the *Right* shows some examples of the quasi-equivalent triangulations of the icosahedron; the colored triangles represent a face of the icosahedra with $T = 3$, 13, and 31 (with total number of particles $n = 32$, 132, and 312, respectively).

charged molecules restricted to shells. Electrostatic interactions organize atomic systems into ionic crystals with an outstanding variety of ordered structures (22, 23). They also drive the ordering of self-assembled systems (1), including cationic–anionic nanoalloys (24), nucleic acids and oppositely charged proteins into toroids (25), and cationic–anionic amphiphiles into vesicles with icosahedral shapes (17).

A particular feature of electrostatically self-assembled systems is that the original spherical symmetry of the Coulomb force usually is broken down to special crystal directions and symmetry planes. We exploit here the way the spherical continuous symmetry of a disordered system is broken by electrostatics, and we use it for icosahedral faceting of a spherical shape. We distribute a set of positive and negative charges over an icosahedron and over a sphere with equal surface area to conserve the total number of particles at different charge stoichiometric ratios. The charges are assumed to interact via a pure Coulombic interaction, plus a short-range hard-core potential. We then determine which structure has the lowest total electrostatic energy.

Results and Discussion

Our model generalizes in two ways the famous Thomson problem (26) (see, for example, refs. 27–30), on how to arrange N electrostatically repulsive particles on a sphere. First, our model is on the icosahedron, not only on the sphere. Second, we consider both negative and positive charges, not only positive ones (the Thomson solution is applicable to a "metallic" bonding assembly where a continuous sea of electrons holds the cations on the surface of the sphere; we consider instead "ionic" bonding among positive and negative ions). Charges distributed on a quasi-equivalent triangulation of the sphere do not always correspond to the lowest energy state, and positional defects proliferate when the number of charges is large. Because our model considers both positive and negative charges, we have ionic conformations that are not equivalent to the Thomson solution (Fig. 2). In our model, there are only 12 5-fold positional defects at the vertices of the icosahedron, whereas internal order (positive–negative) defects are free to proliferate to any degree. After positioning all of the charges over an electroneutral T triangulation, our algorithm swaps them in pairs by using a standard simulated-annealing Metropolis Monte Carlo algorithm, until complete energy relaxation. Because stochastic minimization algorithms can take a long time to find the minimum energy for a large system of charges, we thus corroborate our findings with an auxiliary deterministic minimization method; that is, by adding one charge at a time over the icosahedron and allowing the system to relax (i.e., rearrange the internal order of the charges) at each step. We consider T numbers up to $T = 48$ corresponding to a total number of charges up to $n = 482$. After finding a low energy configuration of charges on the icosahedron, we consider the energy of the same system of charges when projected onto a spherical surface with equal area. However, we do not take a trivial gnomic projection (i.e., purely radial) of the icosahedron over the sphere, because the projection would be oddly distributed on the sphere, with a densely packed region of charges around the vertices of the icosahedron, as shown in Fig. 3. From a physical point of view, short-range interactions tend to distribute the charges at a local scale evenly. We use a more uniform projection by requiring that the area per charge is preserved, namely, the solid angle of any three neighboring charges on the icosahedron is preserved when they are projected onto the sphere, as described in *Materials and Methods*. The validity of such a triangulation of the sphere is based here on plausibility arguments, and it can be verified only by more intensive numerical simulations, such as molecular dynamics.

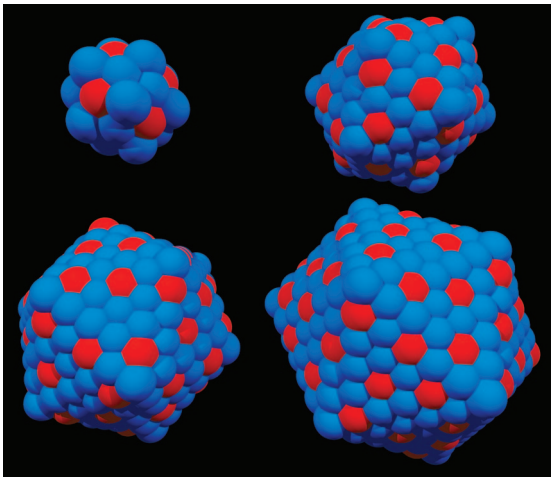

Fig. 2. Examples of charge distributions with spherical topology and icosahedral shape. From right to left, top to bottom, the number of particles N is 32, 132, 212, and 312 (T is 3, 13, 21, and 31), respectively, for 3:1 stoichiometric ratio (+3 charges are red, −1 charges are blue). Note that in the $n = 32$ ($T = 3$) case, the eight "+3" charges are on the vertices of a regular cube and not on a square antiprism as in the Thomson problem for eight charges on a sphere.

The relative difference between the electrostatic energies over the icosahedron and the sphere as a function of the number of charges is shown in Fig. 4. The points below the solid line correspond to systems with icosahedral shapes.

An interesting feature of Fig. 4 is that for the 3:1 and 5:1 cases, the relative energy difference between the spherical and the icosahedral shape is lower for certain T numbers that correspond to T triangulations that have lower bending stiffness. That is, the ionic buckling seems to be controlled by preferred bending directions of the planar ionic structure, along which it is more likely to develop an edge for the icosahedral shape. The ionic buckling is the result of a delicate balance of forces: the electrostatic interactions favor ordered and planar faces that are likely to bend along only a finite set of possible directions. The angles between two edges stemming out from the same vertex are not commensurable with the crystalline bending directions, which generates a distinguishing decoration on the icosahedron faces that breaks the icosahedral symmetry; that is, the faces of the icosahedron are not necessarily equivalent. It therefore is not trivial that there exist configurations preferring icosahedral shapes because only few directions in the ionic lattice facet the sphere. We note that the energy difference between the sphere and the icosahedron depends on the number of particles. Among the stable configurations in Fig. 4, the system will choose the one that takes into account fluctuations of the total number of charges by means of a chemical potential. For an x:1 stoichio-

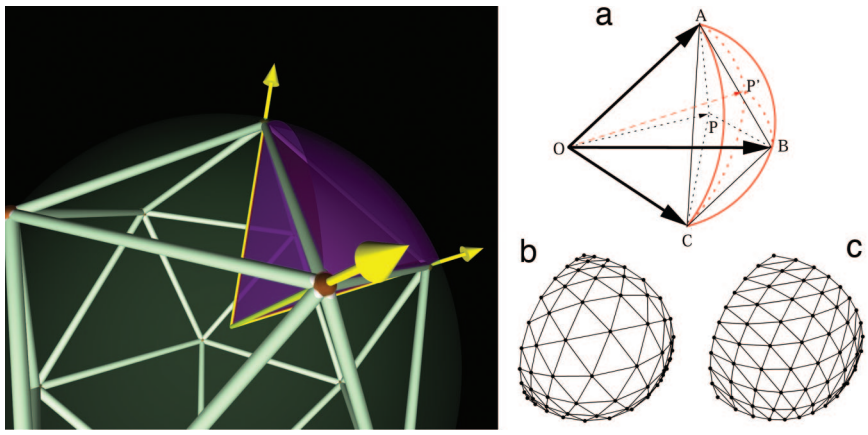

Fig. 3. The projection of an icosahedron onto the sphere is not unique. (*Left*) All of the 20 faces of the icosahedron are projected onto spherical triangles. (*Right*) Every point *P* of the triangular face ABC is mapped onto a point *P′* on the sphere (*a*) (in red). The gnomic projection (*b*) is not as uniform as our equal-area projection (*c*).

metric ratio, fluctuations in the number of charges should occur in clusters of $x + 1$ particles, owing to the electroneutrality condition. This situation is similar to what happens in liquid theory (31). If the chemical potential is such that only small fluctuations in the number of particles are permitted, the icosahedron will be observed for those values of the total number of charges shown in the curves on Fig. 4. However, when large fluctuations in the number of particles are allowed, then it may be possible that the aggregates explore a broad distribution of shapes, both faceted and not faceted. Nevertheless, different types of defects that preserve global electroneutrality (32), such as Frenkel defects (cation-vacancy or cation-interstitial) and Schottky defects (cation-vacancy and anion-vacancy) cannot occur in our case because amphiphilic molecules do not want to expose their tails to water. Therefore, the surface packing in amphiphilic emulsions or membranes tends to be constant (that is, maximal triangular packing). Finally, if there is enough salt in the solution, stoichiometry-breaking defects are possible. However, in the high-salt concentration limit, the electrostatic coassembly of cationic–anionic amphiphiles is not favorable and leads to the dissolution of the aggregate or to macroscopic segregation of the ionic amphiphilic components (15, 17).

Our results for different stoichiometric ratios of charges are collected in Table 1. We note that except for $T\,(1, 1) = 3$ all of the faceted ionic shells have $T(p, q)$ with $p \neq q$, which are chiral structures. Therefore, the charge distribution on the facets breaks chirality besides the other icosahedral symmetries because of the preferred bending directions of an ionic crystalline surface. From Table 1, one can see that there are also spherical distributions of charges that break chirality. Moreover, a direct inspection of the spherical distributions confirms that many other symmetries on the sphere are broken, because of a nonregular arrangement of charges on the spherical surface. The reason is that on the surface one should consider two lattices. The first one is the triangular quasi-equivalent lattice of the positions of the charges, which by definition has only 12 5-fold defects with icosahedral symmetry. The second lattice is the sublattice that is formed by the positive charges only. In general, the two lattices are commensurable on the infinite plane, but they are not commensurable when confined on a surface with spherical topology, as one can see with the following argument *á la* absurdum. Let us assume that the sublattice of positive charges is a valid icosadeltahedral triangulation of the sphere. One could then assign a specific T' number to it. The problem

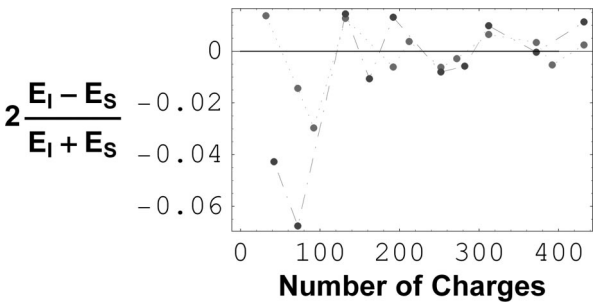

Fig. 4. The relative electrostatic energy difference between icosahedral configurations and spherical configurations versus the total number of charges (3:1 and 5:1 cases, in red and blue, respectively); the points below the solid line correspond to systems with icosahedral shapes.

Table 1. Lowest energy configurations at different stoichiometric ratios

$(h, k) = T$	N	1:1	2:1	3:1	5:1
(1, 0) = 1	12	S	S	S	S
(1, 1) = 3	32	S		I	
(2, 0) = 4	42	S	S		S
(2, 1) = 7	72	S	S	S	S
(3, 0) = 9	92	S		S	
(2, 2) = 12	122	S			
(3, 1) = 13	132	S	S	I	I
(4, 0) = 16	162	S	S		S
(3, 2) = 19	192	S	S	S	I
(4, 1) = 21	212	S		I	
(5, 0) = 25	252	S	S	S	S
(3, 3) = 27	272	S		S	
(4, 2) = 28	282	S	S		S
(5, 1) = 31	312	S	S	I	I
(6, 0) = 36	362	S			
(4, 3) = 37	372	S	S	I	S
(5, 2) = 39	392	S		S	
(6, 1) = 43	432	S	S	I	I
(4, 4) = 48	482	S			

From left to right: *T* number, total number of charges, stoichiometric ratios. An empty entry means the configuration is not allowed because of global electroneutrality. We note that stoichiometric ratios 1:1 and 4:1 form square lattices on a plane, whereas the others form triangular lattices. However, the case 4:1 never fulfills the electroneutrality condition for any given *T* triangulation. The letters "S" and "I" indicate that the most stable structure is the sphere (S) or icosahedron (I), respectively.

of satisfying the constraint of local electroneutrality of the lattice $(x + 1)\ T = T'$, and the global electroneutrality condition $(x + 1)\ N' = N$, where the total number of positive charges is $N' = 10T' + 2$, however, has solution only for very particular cases. Therefore, in general, the positive charges break the whole icosahedral symmetry, both on the icosahedron and on the sphere.

The cases 1:1 and 2:1 are not included in the plot of Fig. 4 because they do not show any electrostatic buckling for the small systems we considered. However, this does not contradict the fact that the buckling of large 1:1 structures, as the ones in ref. 17, can be interpreted by elasticity theory (16). The ionic contribution to the Young's modulus Y for a defectless ionic crystal is such that by increasing the stoichiometric ratio Y increases (33). In other words, the effective Foppl–von Kármán number γ increases with increasing charge per particle, which implies smaller sizes of the buckled surface for larger stoichiometric ratios at low salt concentrations (because Y is expected to decrease with increasing ionic strength). However, we stress that, in general, continuum elastic theory cannot be applied to the small systems where faceting is described by our discrete ionic-driven buckling mechanism.

Finally, one could argue whether the use of a short-range soft potential would change our results. Even if the charged amphiphiles have the same size but finite ionic-core stiffness, the attraction among opposite charges would squeeze the particles together up to a maximum overlap, where the structure again is stabilized by the effective hard-core size. In principle, however, one would have to test this assumption by doing an off-lattice computer simulation. The reorganization of the charges in continuous space rather than on a lattice (as done in this work) might lead to irregular shapes. However, only numerical simulations that include details of the membrane such as the elastic and bending properties could predict them confidently. In the limit of low temperatures (where the number of defects is small) and high chemical potential (where free amphiphilic molecules in solution are energetically unfavorable), our results are still valid because the system must reach the lowest energy state.

Concluding Remarks

The ionic buckling of cationic and anionic shells with small number of particles found here may allow the design of functional materials that can undergo symmetry, shape, and volume changes by controlling the ionic strength of the solution. Namely, at high ionic strengths, the crystalline order is destroyed favoring spherical aggregates, whereas at low ionic strengths we expect buckling. Not all systems with finite number of particles buckle. Buckling seems more probable in chiral ionic shells. Other icosahedral symmetries are broken because of the preferred bending directions of an ionic crystalline surface, resulting in faceted shells without global rotational symmetry. This mechanism may help the design of functional materials that can template the growth and/or orient chains with specific charge sequences. Our results suggest other possible polyhedral shapes in systems where the stoichiometric ratios do not allow triangular lattices, such as the square lattice of a 4:1 stoichiometric ratio. Different surface structures can arise also by changing the size ratio of the components. For example, if the cation to anion ratio is <0.225, then a triangular lattice of anions with a small cation fitting as an interstitial defect in the center of the triangles would form. However, for ratios between 0.225 and 1, more energetically favorable arrangements may exist and possibly not toward an icosahedral faceting. In such cases, a slight out-of-plane packing is possible, and even simple ionic systems may show a large variety of shapes with new symmetries.

It is believed that the first forms of life involved simple closed shapes (34) and/or concentration of molecules with charged groups at liquid–liquid interfaces (35, 36). Our model opens a way to study their possible shapes and symmetries. Symmetries are derived from the fundamental physical properties of the interactions within the system. Our results show that electrostatic interactions are sufficiently robust to generate simple shapes with diverse symmetries.

Materials and Methods

To compute the energy of the icosahedron and compare it with that of a sphere, we use a projection method that imposes that the area per charge is constant when projected onto the sphere as shown in Fig. 3. Consider a point P over a triangular face ABC of the icosahedron (Fig. 3*a*) and its corresponding projected point P'. The position of P can be expressed by its barycentric coordinates α_1, α_2, α_3:

$$P = \sum_{i=1}^{3} \alpha_i \vec{R}_i,\ \vec{R}_1 = \overrightarrow{OA},\ \vec{R}_2 = \overrightarrow{OB},\ \vec{R}_3 = \overrightarrow{OC}, \qquad [1]$$

where α_i are the relative areas of the triangles PCB, PAC, and PBA, respectively, with $\sum_{i=1}^{3} \alpha_i = 1$. Also, the projected point P' can be written as $P' = \sum_{i=1}^{3} \beta_i \vec{R}_i$. The simplest projection is the gnomic projection, which is a purely radial projection over a sphere of radius R leading to $P' = \vec{P}R/|\vec{P}|$. However, such a projection leads to an uneven distribution of points on the sphere (Fig. 3*b*), with densely packed region of charges around the edges and the vertices of the icosahedron. We use a more uniform and physical projection by requiring that the area per charge is preserved. Namely, the solid angle of any three neighboring charges on the icosahedron is preserved by imposing that the relative areas of a point on the triangle ABC (i.e., its barycentric coordinates) are proportional to the relative areas of the corresponding spherical triangle. That is: $\alpha_i = \Omega_i R^2/\Omega_{\mathrm{TOT}} R^2$, where Ω_i are the solid angles between P' and one edge of the spherical triangle ABC. Let $[\vec{a}, \vec{b}, \vec{c}]$ be the triple vector product of three vectors $\vec{a}, \vec{b}, \vec{c}$. The solid angles Ω_i can then be obtained by the formula (37):

$$\tan\frac{\Omega_1}{2} = \frac{[\vec{P}', \vec{R}_2, \vec{R}_3]}{R^3 + (\vec{R}_2 \cdot \vec{R}_3)\vec{P}' + (\vec{R}_3 \cdot \vec{P}')\vec{R}_2 + (\vec{P}' \cdot \vec{R}_2)\vec{R}_3} \qquad [2]$$

and the two similar formulas that are obtained by cyclic permutations (for the spherical triangles BAP′, ACP′, CBP′). By substituting the definition $\sum_{i=1}^{3} \beta_i \vec{R}_i$, and by using basic geometrical properties of the icosahedron, one can solve the linear system of equations for β_i, as a function of the α_i. Finally, the results are homogenously scaled by a factor λ such that the total area of the sphere is equal to the total area of the icosahedron (an "equal-area" spherical projection is shown in Fig. 3*c*). We then relax the system of charges over the sphere with a series of simulated annealing Monte Carlo sweeps. Fig. 1 shows a snapshot of a typical distribution of charges on the sphere and the icosahedron (case 3:1).

We thank Megan Greenfield, Alfonso Mondragón, and Samuel Stupp for helpful discussions. This work was supported by National Science Foundation Grants EEC-0647560 and DMR-0414446.

1. Whitesides GM, Grzybowski B (2002) *Science* 295:2418–2421.
2. Chandler D (2005) *Nature* 437:640–647.
3. Karin M (2006) *Nature* 443:508–509.
4. Marks LD (1994) *Rep Prog Phys* 57:603–649.
5. Caspar DLD, Klug A (1962) *Cold Spring Harbor Symp Quant Biol* 27:1–24.
6. Soderman O, Herrington KL, Kaler EW, Miller DD (1997) *Langmuir* 13:5531–5538.
7. Lin Z, He M, Scriven LE, Davis HT, Snow SA (1993) *J Phys Chem* 97:3571–3578.
8. Mason TG, Wilking JN, Meleson K, Chang CB, Graves SM (2006) *J Phys Condens Mat* 18:R635–R666.

9. Bug ALR, Cates ME, Safran ALR, Witten TA (1987) *J Chem Phys* 87:1824–1833.
10. Guerin CBE, Szleifer I (1999) *Langmuir* 15:7901–7911.
11. Cech TR, Bass BL (1986) *Annu Rev Biochem* 55:599–629.
12. Huang C, Olvera de la Cruz M, Swift BW (1995) *Macromolecules* 28:7996–8005.
13. Goldar A, Sikorav JL (2004) *Eur Phys J E* 14:211–239.
14. Loverde SM, Velichko YS, Olvera de la Cruz M (2006) *J Chem Phys* 124:144702.
15. Solis FJ, Stupp SI, Olvera de la Cruz M (2005) *J Chem Phys* 122:54905.
16. Lidmar J, Mirny L, Nelson. DR (2003) *Phys Rev E Stat Nonlin Soft Matter Phys* 68:051910.
17. Dubois M, Deme B, Gulik-Krzywicki T, Dedieu JC, Vautrin C, Desert S, Perez E, Zemb T (2001) *Nature* 411:672–675.
18. Chen T, Zhang ZL, Glotzer SC (2007) *Proc Natl Acad Sci USA* 104:717–722.
19. Zandi R, Reguera D, Bruinsma RF, Gelbart WM, Rudnick J (2004) *Proc Natl Acad Sci USA* 101:15556–15560.
20. Seung HS, Nelson DR (1988) *Phys Rev A* 38:1005–1018.
21. Witten TA, Li H (1993) *Europhys Lett* 23:51–55.
22. Hone D, Alexander S, Chaikin PM, Pincus P (1983) *J Chem Phys* 79:1474–1479.
23. Yan QL, de Pablo JJ (2002) *Phys Rev Lett* 88:095504.
24. Kalsin AM, Fialkowski M, Paszewski M, Smoukov SK, Bishop KJM, Grzybowski BA (2006) *Science* 312:420–424.
25. Raspaud E, M. Olvera de la Cruz, Sikorav JL, Livolant F (1998) *Biophys J* 74:381–393.
26. Thomson JJ (1904) *Philos Mag* 7:237–265.
27. Bowick MJ, Cacciuto A, Nelson DR, Travesset A (2006) *Phys Rev B* 73:024115.
28. Altschuler EL, Perez-Garrido A (2006) *Phys Rev E Stat Nonlin Soft Matter Phys* 73:036108.
29. Einert T, Lipowsky P, Schilling J, Bowick MJ, Bausch AR (2005) *Langmuir* 21:12076–12079.
30. Travesset A (2005) *Phys Rev E Stat Nonlin Soft Matter Phys* 72:036110.
31. Greberg H, Kjellander R, Akesson T (1996) *Mol Phys* 87:407–422.
32. Kotomin EA, Puchin VE, Jacobs PWM (1993) *Philos Mag A* 68:1359–1367.
33. Green DJ (1998) *An Introduction to the Mechanical Properties of Ceramics* (Cambridge Univ Press, Cambridge, UK).
34. Szostak JW, Bartel DP, Luisi PL (2001) *Nature* 409:387–390.
35. Onsager L (1973) in *Coral Gables Conference*, eds Mintz SL, Widmayer SM (Plenum Press, New York), p 1.
36. Oparin AI (1965) *Adv Enzymol* 27:347–380.
37. Vanoosterom A, Strackee J (1983) *IEEE Trans Biomed Engin* 30:125–126.